

Chemo–Dynamical SPH code for evolution of star forming disk galaxies.

Peter Berczik

Main Astronomical Observatory of Ukrainian National Academy of Sciences, 252650, Golosiiv, Kiev-022, Ukraine
e-mail: berczik@mao.kiev.ua

Received: 16 February, 1999 / Accepted: 30 April, 1999

Abstract. A new Chemo–Dynamical Smoothed Particle Hydrodynamic (CD-SPH) code is presented. The disk galaxy is described as a multi–fragmented gas and star system, embedded in a cold dark matter halo with a rigid potential field. The star formation (SF) process, SNII, SNIa and PN events, and the chemical enrichment of gas, have all been considered within the framework of the standard SPH model, which we use to describe the dynamical and chemical evolution of triaxial disk–like galaxies. It is found that such approach provides a realistic description of the process of formation, chemical and dynamical evolution of disk galaxies over a cosmological timescale.

Key words: chemical and dynamical evolution of disk galaxies – CD-SPH – star formation in SPH

1. Introduction

The dynamical and chemical evolution of galaxies is one of the most interesting and complex of problems. Naturally, galaxy formation is closely connected with the process of large–scale structure formation in the Universe.

The main role in the scenario of large–scale structure formation seems to be played by the dark matter. It is believed that the Universe was seeded at some early epoch with low density fluctuations of dark non–baryonic matter, and the evolving distribution of these dark halos provides the arena for galaxy formation. Galaxy formation itself involves collapse of baryons within potential wells of dark halos (White & Rees 1978). The properties of forming galaxies depend on the amount of baryonic matter that can be accumulated in such halos and the efficiency of star formation. The observational support for this galaxy formation scenario comes from the recent COBE detection of fluctuations in the microwave background (*e.g.* Bennett *et al.* 1993).

Send offprint requests to: Peter Berczik

The investigation of galaxy formation is a highly complex subject requiring many different approaches. The formation of self–gravitating inhomogeneities of protogalactic size, the ratio of baryonic and non–baryonic matter (Bardeen *et al.* 1986; White & Silk 1979; Peebles 1993; Dar 1995), the origin of the protogalaxy’s initial angular momentum (Voglis & Hiotelis 1989; Zurek *et al.* 1988; Eisenstein & Loeb 1995; Steinmetz & Bartelmann 1995), and the protogalaxy’s collapse and its subsequent evolution are all usually considered as separate problems. Recent advances in computer technology and numerical methods have allowed detailed modeling of baryon matter dynamics in the universe dominated by collisionless dark matter and, therefore, the detailed gravitational and hydrodynamical description of galaxy formation and evolution. The most sophisticated models include radiative processes, star formation and supernova feedback (*e.g.* Katz 1992; Steinmetz & Muller 1994; Friedli & Benz 1995).

The results of numerical simulations are essentially affected by the star formation algorithm incorporated into modeling techniques. The star formation and related processes are still not well understood on either small or large spatial scales, such that the star formation algorithm by which the gas material is converted into stars can only be based on simple theoretical assumptions or on empirical observations of nearby galaxies. The other most important effect of star formation on the global evolution of a galaxy is caused by a large amount of energy released in supernova explosions and stellar winds.

Among numerous methods developed for the modeling of complex three dimensional hydrodynamic phenomena, Smoothed Particle Hydrodynamics (SPH) is one of the most popular (Monaghan 1992). Its Lagrangian nature allows easy combination with fast N–body algorithms, making it suitable for simultaneous description of the complex dynamics of a gas–stellar system (Friedli & Benz 1995). As an example of such a combination, the TREE-SPH code (Hernquist & Katz 1989; Navarro & White 1993)

was successfully applied to the detailed modeling of disk galaxy mergers (Mihos & Hernquist 1996) and of galaxy formation and evolution (Katz 1992). The second good example is a GRAPE-SPH code (Steinmetz & Muller 1994; Steinmetz & Muller 1995) which was successfully used to model the evolution of disk galaxy structure and kinematics.

In recent years, there have been excellent papers concerning the complex SPH modeling of galaxy formation and evolution (Raiteri *et al.* 1996; Carraro *et al.* 1997). Our code, proposes new "energetic" criteria for SF, and suggest a more realistic account of returned chemically enriched gas fraction via SNII, SNIa and PN events.

The simplicity and numerical efficiency of the SPH method were the main reasons why we chose this technique for the modeling of the evolution of complex, multi-fragmented triaxial protogalactic systems. We used our own modification of the hybrid N-body/SPH method (Berczik & Kravchuk 1996; Berczik 1998), which we call the chemo–dynamical SPH (CD-SPH) code.

The "dark matter" and "stars" are included in the standard SPH algorithm as the N-body collisionless system of particles, which can interact with the gas component only through gravitation (Katz 1992). The star formation process and supernova explosions are also included in the scheme as proposed by Raiteri *et al.* (1996), but with our own modifications.

2. The CD-SPH code

2.1. The SPH code

Continuous hydrodynamic fields in SPH are described by the interpolation functions constructed from the known values of these functions at randomly positioned particles (Monaghan 1992). Following Monaghan & Lattanzio (1985) we use for the kernel function W_{ij} the spline expression in the form of:

$$W_{ij} = \frac{1}{\pi h^3} \begin{cases} 1 - \frac{3}{2}u_{ij}^2 + \frac{3}{4}u_{ij}^3, & \text{if } 0 \leq u_{ij} < 1, \\ \frac{1}{4}(2 - u_{ij})^3, & \text{if } 1 \leq u_{ij} < 2, \\ 0, & \text{otherwise.} \end{cases} \quad (1)$$

Here $u_{ij} = r_{ij}/h$.

To achieve the same level of accuracy for all points in the fluid, it is necessary to use a spatially variable smoothing length. In this case each particle has its individual value of h . Following Hernquist & Katz (1989), we write:

$$\langle \rho(\mathbf{r}_i) \rangle = \sum_{j=1}^N m_j \cdot \frac{1}{2} \cdot [W(r_{ij}; h_i) + W(r_{ij}; h_j)]. \quad (2)$$

In our calculations the values of h_i were determined from the condition that the number of particles N_B in the

neighborhood of each particle within the $2 \cdot h_i$ remains constant (Mihos & Hernquist 1996). The value of N_B is chosen such that a certain fraction of the total number of "gas" particles N affects the local flow characteristics (Hiotelis & Voglis 1991). If the defined h_i becomes smaller than the minimal smoothing length h_{min} , we set the value $h_i = h_{min}$. For "dark matter" and "star" particles (with Plummer density profiles) we use, accordingly, the fixed gravitational smoothing lengths h_{dm} and h_{star} .

If the density is computed according to Equation (2), then the continuity equation is satisfied automatically. Equations of motion for particle i are

$$\frac{d\mathbf{r}_i}{dt} = \mathbf{v}_i, \quad (3)$$

$$\frac{d\mathbf{v}_i}{dt} = -\frac{\nabla_i P_i}{\rho_i} + \mathbf{a}_i^{vis} - \nabla_i \Phi_i - \nabla_i \Phi_i^{ext}, \quad (4)$$

where P_i is the pressure, Φ_i is the self gravitational potential, Φ_i^{ext} is a gravitational potential of possible external halo and \mathbf{a}_i^{vis} is an artificial viscosity term (Hiotelis *et al.* 1991). The energy equation has the form:

$$\frac{du_i}{dt} = -\frac{P_i}{\rho_i} \nabla_i \mathbf{v}_i + \frac{\Gamma_i - \Lambda_i}{\rho_i}. \quad (5)$$

Here u_i is the specific internal energy of particle i . The term $(\Gamma_i - \Lambda_i)/\rho_i$ accounts for non adiabatic processes not associated with the artificial viscosity (in our calculations $\Gamma_i \equiv 0$). We present the radiative cooling in the form:

$$\Lambda_i = \Lambda_i(u_i, \rho_i) = \Lambda_i^*(T_i) \cdot n_i^2, \quad (6)$$

where n_i is the hydrogen number density and T_i the temperature. To follow its subsequent thermal behaviour in numerical simulations, we use an analytical approximation of the standard cooling function $\Lambda^*(T)$ for an optically thin primordial plasma in ionization equilibrium (Dalgarno & McCray 1972; Katz & Gunn 1991). Its absolute cutoff temperature is set equal to 10^4 K.

The equation of state must be added to close the system.

$$P_i = \rho_i \cdot (\gamma - 1) \cdot u_i, \quad (7)$$

where $\gamma = 5/3$ is the adiabatic index.

2.2. Time integration

To solve the system of Equations (3), (4) and (5) we use the leapfrog integrator (Hernquist & Katz 1989). The time step δt_i for each particle depends on the particle's acceleration \mathbf{a}_i and velocity \mathbf{v}_i , as well as on viscous forces. To define δt_i we use the relation from Hiotelis & Voglis (1991), and adopt Courant's number $C_n = 0.1$.

We carried out (Berczik & Kolesnik 1993) a large series of test calculations to check that the code is correct, the conservation laws are obeyed and the hydrodynamic fields are represented adequately, all with good results.

2.3. The star formation algorithm

It is well known that star formation (SF) regions are associated with giant molecular complexes, especially with regions that are approaching dynamical instability. The early phase of star formation does not seem to crucially affect the dynamics of a galaxy. From the beginning of the collapse, such a system decouples from its surroundings and evolves on a completely different timescale. When the chemically enriched gas content of the galaxy decreases, the heating by winds and supernova explosions (Leitherer *et al.* 1992) begins to play an important role in the dynamics of the galaxy. The overall picture of star formation seems to be understood, but the detailed physics of star formation and accompanying processes, on either small or large scales, remains sketchy (Larson 1969; Silk 1987).

All the above stated as well as computer constraints cause the using of simplified numerical algorithms of description of conversion of the gaseous material into stars, which are based on simple theoretical assumptions and/or on results of observations of nearby galaxies.

To describe of the process of converting of gaseous material into stars we modify the standard SPH star formation algorithm (Katz 1992; Navarro & White 1993), taking into account the presence of random motions in the gaseous environment and the time lag between the initial development of suitable conditions for star formation and star formation itself (Berczik & Kravchuk 1996; Berczik 1998). The first reasonable requirement incorporated into this algorithm allows selecting "gas" particles that are potentially eligible to form stars. It states that in the separate "gas" particle the SF can start if the absolute value of the "gas" particle's gravitational energy exceeds the sum of its thermal energy and the energy of random motions:

$$|E_i^{gr}| > E_i^{th} + E_i^{ch}. \quad (8)$$

Gravitational and thermal energies and the energy of random motions for the "gas" particle i in model simulation are defined as:

$$\begin{cases} E_i^{gr} = -\frac{3}{5} \cdot G \cdot m_i^2 / h_i, \\ E_i^{th} = \frac{3}{2} \cdot m_i \cdot c_i^2, \\ E_i^{ch} = \frac{1}{2} \cdot m_i \cdot \Delta v_i^2, \end{cases} \quad (9)$$

where $c_i = \sqrt{\mathcal{R} \cdot T_i / \mu}$ is the isothermal sound speed of particle i . We set $\mu = 1.3$ and define the random or "turbulent" square velocities near particle i as:

$$\Delta v_i^2 = \sum_{j=1}^{N_B} m_j \cdot (\mathbf{v}_j - \mathbf{v}_c)^2 / \sum_{j=1}^{N_B} m_j, \quad (10)$$

where:

$$\mathbf{v}_c = \sum_{j=1}^{N_B} m_j \cdot \mathbf{v}_j / \sum_{j=1}^{N_B} m_j. \quad (11)$$

For practical reasons, it is useful to define a critical temperature for SF onset in particle i as:

$$T_i^{crit} = \frac{\mu}{3\mathcal{R}} \cdot \left(\frac{8}{5} \cdot \pi \cdot G \cdot \rho_i \cdot h_i^2 - \Delta v_i^2 \right). \quad (12)$$

Then, if the temperature of the "gas" particle i , drops below the critical one, SF can proceed.

$$T_i < T_i^{crit}. \quad (13)$$

We think that requirement (8), or in another form (13), is the only one needed. It seems reasonable that the chosen "gas" particle will produce stars only if the above condition hold over the interval that exceeds its free - fall time $t_{ff} = \sqrt{3 \cdot \pi / (32 \cdot G \cdot \rho)}$. This condition is based on the well known fact that, due to gravitational instability, all substructures of a collapsing system are formed on such a timescale. Using it, we exclude transient structures, that are destroyed by the tidal action of surrounding matter from consideration.

We also define which "gas" particles remain cool, *i.e.* $t_{cool} < t_{ff}$. We rewrite this condition as presented in Navarro & White (1993): $\rho_i > \rho_{crit}$. Here we use the value of $\rho_{crit} = 0.03 \text{ cm}^{-3}$.

When the collapsing particle i is defined, we create the new "star" particle with mass m^{star} and update the "gas" particle m_i using these simple equations:

$$\begin{cases} m^{star} = \epsilon \cdot m_i, \\ m_i = (1 - \epsilon) \cdot m_i. \end{cases} \quad (14)$$

Here ϵ , defined as the global efficiency of star formation, is the fraction of gas converted into stars according to the appropriate initial mass function (IMF). The typical values for SF efficiency in our Galaxy on the scale of giant molecular clouds are in the range $\epsilon \approx 0.01 \div 0.4$ (Duerr *et al.* 1982; Wilking & Lada 1983). But it is still a little known quantity. In numerical simulation the model parameter has to be checked by comparison of numerical simulation results with available observational data. Here we define ϵ as:

$$\epsilon = 1 - (E_i^{th} + E_i^{ch}) / |E_i^{gr}|, \quad (15)$$

with the requirement that all excess mass of the gas component in a star-forming particle, which provides the inequality $|E_i^{gr}| > E_i^{th} + E_i^{ch}$, is transformed into the star component. In the code we set the absolute maximum value of the mass of such a "star" particle $m_{max}^{star} = 2.5 \cdot 10^6 M_\odot$ *i.e.* $\approx 5\%$ of the initial particle mass m_i .

At the moment of stellar birth, the position and velocities of new "star" particles are equal to those of parent "gas" particles. Thereafter these "star" particles interact with other "gas", "star" or "dark matter" particles only by gravitation. The gravitational smoothing length for these (Plummer like) particles is set equal to h_{star} .

2.4. The thermal SNII feed-back

We try to include the events of SNII, SNIa and PN in the complex gasdynamic picture of galaxy evolution. But, for the thermal budget of the ISM, only SNII plays the main role. Following Katz (1992), we assume that the explosion energy is converted totally into thermal energy. The stellar wind action seems not to be essential in the energy budget (Ferriere 1995). The total energy released by SNII explosions (10^{44} J per SNII) within a "star" particle is calculated at each time step and distributed uniformly between the surrounding (*i.e.* $r_{ij} < h_{star}$) "gas" particles (Raiteri *et al.* 1996).

2.5. The chemical enrichment of gas

Every "star" particle in our SF scheme represents a separate, gravitationally closed star formation macro region (like a globular cluster). The "star" particle is characterized by its own time of birth t_{begSF} which is set equal to the moment of particle formation. After the formation, these particles return the chemically enriched gas into surrounding "gas" particles due to SNII, SNIa and PN events. For the description of this process we use the approximation proposed by Raiteri *et al.* (1996). We consider only the production of ^{16}O and ^{56}Fe , and try to describe the full galactic time evolution of these elements, from the beginning to present time (*i.e.* $t_{evol} \approx 13.0$ Gyr).

With the multi-power IMF law suggested by Kroupa *et al.* (1993), the distribution of stellar masses within a "star" particle of mass m^{star} is then:

$$\Psi(m) = m^{star} \cdot A \cdot \begin{cases} 2^{0.9} \cdot m^{-1.3}, & \text{if } 0.1 \leq m < 0.5, \\ m^{-2.2}, & \text{if } 0.5 \leq m < 1.0, \\ m^{-2.7}, & \text{if } 1.0 \leq m, \end{cases} \quad (16)$$

where m is the star mass in solar units. With adopted lower ($m_{low} = 0.1 M_{\odot}$) and upper ($m_{upp} = 100 M_{\odot}$) limits of the IMF, the normalization constant $A \approx 0.31$.

For the definition of stellar lifetimes we use the equation (Raiteri *et al.* 1996):

$$\log t_{dead} = a_0(Z) - a_1(Z) \cdot \log m + a_2(Z) \cdot (\log m)^2, \quad (17)$$

where t_{dead} is expressed in years, m is in solar units, and coefficients are defined as:

$$\begin{cases} a_0(Z) = 10.130 + 0.0755 \cdot \log Z - 0.0081 \cdot (\log Z)^2, \\ a_1(Z) = 4.4240 + 0.7939 \cdot \log Z + 0.1187 \cdot (\log Z)^2, \\ a_2(Z) = 1.2620 + 0.3385 \cdot \log Z + 0.0542 \cdot (\log Z)^2. \end{cases} \quad (18)$$

These relations are based on the calculations of the Padova group (Alongi *et al.* 1993; Bressan *et al.* 1993; Bertelli *et al.* 1994) and give a reasonable approximation to stellar lifetimes in the mass range from $0.6 M_{\odot}$ to $120 M_{\odot}$ and metallicities $Z = 7 \cdot 10^{-5} \div 0.03$ (defined as a mass of all elements heavier than He). In our calculation following Raiteri *et al.* (1996), we assume that Z scales with the oxygen abundance as $Z/Z_{\odot} = ^{16}\text{O}/^{16}\text{O}_{\odot}$. For those metallicities exceeding available data we take the value corresponding to the extremes.

We can define the number of SNII explosions inside a given "star" particle during the time from t to $t + \Delta t$ using a simple equation:

$$\Delta N_{\text{SNII}} = \int_{m_{dead}(t+\Delta t)}^{m_{dead}(t)} \Psi(m) dm, \quad (19)$$

where $m_{dead}(t)$ and $m_{dead}(t + \Delta t)$ are masses of stars that end their lifetimes at the beginning and at the end of the respective time step. We assume that all stars with masses between $8 M_{\odot}$ and $100 M_{\odot}$ produce SNII, for which we use the yields from Woosley & Weaver (1995). The approximation formulae from Raiteri *et al.* (1996) defines the total ejected mass by one SNII - m_{ej}^{tot} , as well as the ejected mass of iron - m_{ej}^{Fe} and oxygen - m_{ej}^{O} as a function of stellar mass (in solar units).

$$\begin{cases} m_{ej}^{tot} = 7.682 \cdot 10^{-1} \cdot m^{1.056}, \\ m_{ej}^{\text{Fe}} = 2.802 \cdot 10^{-4} \cdot m^{1.864}, \\ m_{ej}^{\text{O}} = 4.586 \cdot 10^{-4} \cdot m^{2.721}. \end{cases} \quad (20)$$

To take into account PN events inside the "star" particle we use the equation, as for (19):

$$\Delta N_{\text{PN}} = \int_{m_{dead}(t+\Delta t)}^{m_{dead}(t)} \Psi(m) dm. \quad (21)$$

Following van den Hoek & Groenewegen (1997), Samland (1997) and Samland *et al.* (1997), we assume that all stars with masses between $1 M_{\odot}$ and $8 M_{\odot}$ produce PN. We define the average ejected masses (in solar units) of one PN event as (Renzini & Voli 1981; van den Hoek & Groenewegen 1997):

$$\begin{cases} m_{ej}^{tot} = 1.63, \\ m_{ej}^{Fe} = 0.00, \\ m_{ej}^O = 0.00. \end{cases} \quad (22)$$

The method described in Raiteri *et al.* (1996) and proposed in Greggio & Renzini (1983) and Matteuchi & Greggio (1986) is used to account for SNIa. In simulations, the number of SNIa exploding inside a selected "star" particle during each time step is given by:

$$\Delta N_{\text{SNIa}} = \int_{m_{\text{dead}}(t+\Delta t)}^{m_{\text{dead}}(t)} \Psi_2(m_2) dm_2. \quad (23)$$

The quantity $\Psi_2(m_2)$ represents the initial mass function of the secondary component and includes the distribution function of the secondary's mass relative to the total mass of the binary system m_B ,

$$\Psi_2(m_2) = m^{star} \cdot A_2 \cdot \int_{m_{inf}}^{m_{sup}} \left(\frac{m_2}{m_B}\right)^2 \cdot m_B^{-2.7} dm_B, \quad (24)$$

where $m_{inf} = \max(2 \cdot m_2, 3 M_\odot)$ and $m_{sup} = m_2 + 8 M_\odot$. Following van den Berg & McClure (1994) the value of normalization constant we set, equal to $A_2 = 0.16 \cdot A$.

The total ejected mass (in solar units) is (Thielemann *et al.* 1986; Nomoto *et al.* 1984):

$$\begin{cases} m_{ej}^{tot} = 1.41, \\ m_{ej}^{Fe} = 0.63, \\ m_{ej}^O = 0.13. \end{cases} \quad (25)$$

In summary, a new "star" particle (with metallicity $Z = 10^{-4}$) with mass $10^4 M_\odot$ during the total time of evolution t_{evol} produces:

$$\Delta N_{\text{SNII}} \approx 52.5, \quad \Delta N_{\text{PN}} \approx 1770.0, \quad \Delta N_{\text{SNIa}} \approx 8.48.$$

Fig. 1. presents the number of SNII, SNIa and PN events for this "star" particle.

In Fig. 2. and Fig. 3. we present the returned masses of ^{56}Fe and ^{16}O . We can estimate the total masses (H, He, ^{56}Fe , ^{16}O) (in solar masses) returned to the surrounding "gas" particles due to these processes as:

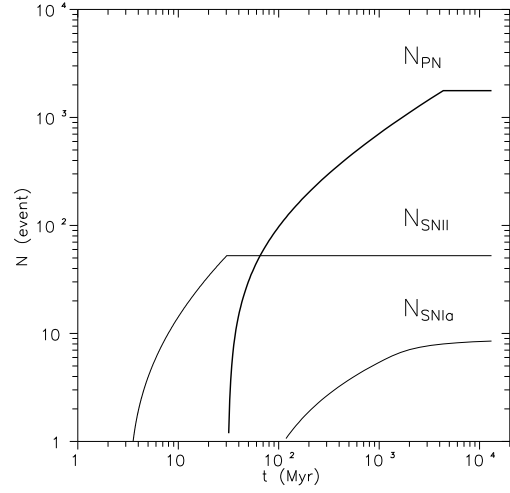


Fig. 1. The number of SNII, SNIa and PN events

$$\begin{cases} \Delta m_{\text{SNII}}^{\text{H}} = 477, & \Delta m_{\text{PN}}^{\text{H}} = 2164, & \Delta m_{\text{SNIa}}^{\text{H}} = 4.14, \\ \Delta m_{\text{SNII}}^{\text{He}} = 159, & \Delta m_{\text{PN}}^{\text{He}} = 721.3, & \Delta m_{\text{SNIa}}^{\text{He}} = 1.38, \\ \Delta m_{\text{SNII}}^{\text{Fe}} = 3.5, & \Delta m_{\text{PN}}^{\text{Fe}} = 0.000, & \Delta m_{\text{SNIa}}^{\text{Fe}} = 5.35, \\ \Delta m_{\text{SNII}}^{\text{O}} = 119, & \Delta m_{\text{PN}}^{\text{O}} = 0.000, & \Delta m_{\text{SNIa}}^{\text{O}} = 1.10. \end{cases} \quad (26)$$

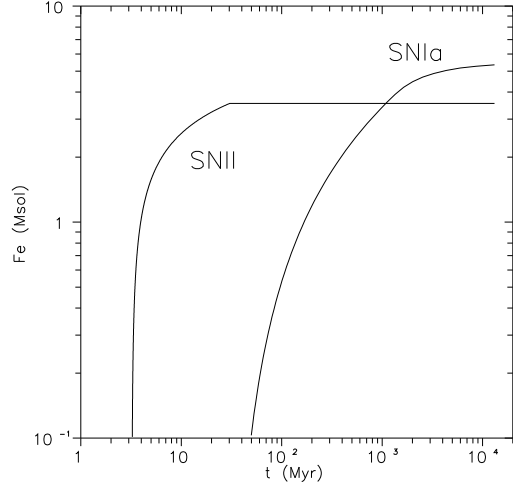


Fig. 2. The returned mass of ^{56}Fe

2.6. The cold dark matter halo

In the literature we have found some profiles, sometimes controversial, for the galactic Cold Dark Matter Haloes (CDMH) (Burkert 1995; Navarro 1998). For resolved structures of CDMH: $\rho_{halo}(r) \sim r^{-1.4}$

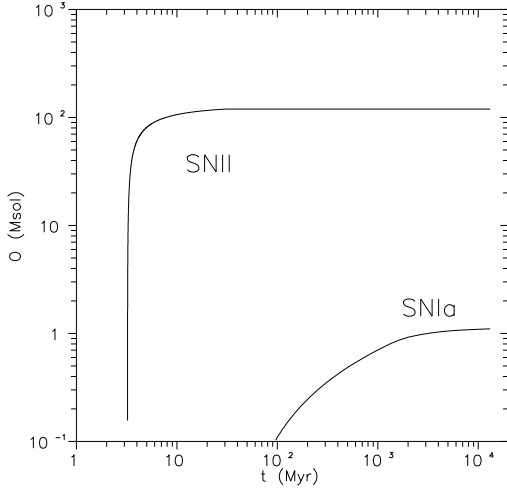


Fig. 3. The returned mass of ^{16}O

(Moore *et al.* 1997). The structure of CDMH high-resolution N-body simulations can be described by: $\rho_{\text{halo}}(r) \sim r^{-1}$ (Navarro *et al.* 1996; Navarro *et al.* 1997). Finally, in Kravtsov *et al.* (1997), we find that the cores of DM dominated galaxies may have a central profile: $\rho_{\text{halo}}(r) \sim r^{-0.2}$.

In our calculations and as a first approximation, it is assumed that the model galaxy halo contains the CDMH component with Plummer - type density profiles (Doughole & Colin 1995):

$$\rho_{\text{halo}}(r) = \frac{M_{\text{halo}}}{\frac{4}{3}\pi b_{\text{halo}}^3} \cdot \frac{b_{\text{halo}}^5}{(r^2 + b_{\text{halo}}^2)^{\frac{5}{2}}}, \quad (27)$$

Therefore for the external force acting on the "gas" and "star" particles we can write:

$$-\nabla_i \Phi_i^{\text{ext}} = -G \cdot \frac{M_{\text{halo}}}{(r_i^2 + b_{\text{halo}}^2)^{\frac{3}{2}}} \cdot \mathbf{r}_i. \quad (28)$$

3. Results and discussion

3.1. Initial conditions

After testing our code demonstrated that simple assumptions can lead to a reasonable model of a galaxy. The SPH calculations were carried out for $N_{\text{gas}} = 2109$ "gas" particles. According to Navarro & White (1993) and Raiteri *et al.* (1996), such a number seems adequate for a qualitatively correct description of the systems behaviour. Even this small a number of "gas" particles produces $N_{\text{star}} = 31631$ "star" particles at the end of the calculation.

The value of the smoothing length h_i was chosen to require that each "gas" particle had $N_B = 21$ neighbors within $2 \cdot h_i$. Minimal h_{min} was set equal to 1 kpc, and the fixed gravitational smoothing length $h_{\text{star}} = 1$ kpc was used for the "star" particles. Our results show that

a value of $N_B \approx 1\% N_{\text{gas}}$ provides qualitatively correct treatment of the system's large scale evolution.

As the initial model (relevant for CDM - scenario) we took a constant-density homogeneous gaseous triaxial configuration ($M_{\text{gas}} = 10^{11} M_{\odot}$) within the dark matter halo ($M_{\text{halo}} = 10^{12} M_{\odot}$). We set $A = 100$ kpc, $B = 75$ kpc and $C = 50$ kpc for semiaxes of system. Such triaxial configurations are reported in cosmological simulations of the dark matter halo formation (Eisenstein & Loeb 1995; Frenk *et al.* 1988; Warren *et al.* 1992). Initially, the centers of all particles were placed on a homogeneous grid inside this triaxial configuration. We set the smoothing parameter of CDMH: $b_{\text{halo}} = 25$ kpc. These values of M_{halo} and b_{halo} are typical for CDMH in disk galaxies (Navarro *et al.* 1996; Navarro *et al.* 1997; Burkert 1995).

The gas component was assumed to be cold initially, $T_0 = 10^4$ K. As we see in our calculations, the influence of random motions essentially reduces the dependence of model parameters on the adopted temperature cutoff and, therefore, on the adopted form of the cooling function itself.

The gas was assumed to be involved in the Hubble flow ($H_0 = 65$ km/s/Mpc) and the solid - body rotation around z - axis. We added small random velocity components ($\Delta |\mathbf{v}| = 10$ km/s) to account for the random motions of fragments. The initial velocity field was defined as:

$$\mathbf{v}(x, y, z) = [\boldsymbol{\Omega}(x, y, z) \times \mathbf{r}] + H_0 \cdot \mathbf{r} + \Delta \mathbf{v}(x, y, z), \quad (29)$$

where $\boldsymbol{\Omega}(x, y, z)$ is the angular velocity of an initially rigidly rotating system.

The spin parameter in our numerical simulations is $\lambda \approx 0.08$, defined in Peebles (1969) as:

$$\lambda = \frac{|\mathbf{L}_0| \cdot \sqrt{|E_0^{gr}|}}{G \cdot (M_{\text{gas}} + M_{\text{halo}})^{5/2}}, \quad (30)$$

\mathbf{L}_0 is the total initial angular momentum and E_0^{gr} is the total initial gravitational energy of a protogalaxy. It is to be noted that for a system in which angular momentum is acquired through the tidal torque of the surrounding matter, the standard spin parameter does not exceed $\lambda \approx 0.11$ (Steinmetz & Bartelmann 1995). Moreover, its typical values range between $\lambda \approx 0.07_{-0.05}^{+0.04}$, e.g. $0.02 \leq \lambda \leq 0.11$.

3.2. Dynamical model

In Fig. 4. we present the "XY", "XZ" and "YZ" distributions of "gas" particles at the final time step ($t_{\text{evol}} \approx 13.0$ Gyr). The box size is 50 kpc. In Fig. 5. we present the distributions of "star" particles. The "star" distributions have dimensions typical of a disk galaxy. The radial extension is approximately 25 – 30 kpc. The disk height is around 1 – 2 kpc. In the center the "bar-like" structure is developed as a result of strong initial triaxial structure

whole in the plane of the disk we can see the "spiral - like" distribution of particles, with extended arm filaments. The "gas" particles are located within central 5 – 10 kpc.

Except for the central region (< 2 kpc), the gas distribution has an exponential form with radial scale length ≈ 2.8 kpc. The column density distributions of gas $\sigma_{gas}(r)$ and stars $\sigma_*(r)$ are presented in Fig. 6. The total column density is defined as: $\sigma_{tot}(r) = \sigma_{gas}(r) + \sigma_*(r)$. The total column density distribution $\sigma_{tot}(r)$ is well approximated (in the interval from 5 kpc to 15 kpc) with an exponential profile characterized by a ≈ 3.5 kpc radial scale length. This value is very close to one reported recently (3.5 kpc) for the radial scale length of the total disk mass surface density distribution obtained for our Galaxy (Mera *et al.* 1998b). The value of $\sigma_{tot} \approx 55 M_\odot \text{pc}^{-2}$ near the location of the Sun ($r \approx 9$ kpc) is close to a recent determination of the total density $52 \pm 13 M_\odot \text{pc}^{-2}$ (Mera *et al.* 1998a).

Fig. 7. shows both the rotational velocity distribution of gas $V_{rot}(r)$ resulting from the modeled disk galaxy calculation and the rotational curve for our Galaxy (Vallee 1994), both of which are very close.

The gaseous radial $V_{rad}(r)$ and normal $V_z(r)$ velocity distributions are in Fig. 8. and Fig. 9. The radial velocity dispersion has a maximum value ≈ 60 km/s in the center, a high value mainly caused by the central strong bar structure. Near the Sun this dispersion drops down to ≈ 20 km/s. Such radial dispersion is reported in the kinematic study of the stellar motions in the solar neighborhood (Bienayme 1998), while the normal dispersion is near ≈ 20 km/s in the whole disk. This value also coincides with the vertical dispersion velocity near the Sun (Bienayme 1998).

We present the temperature distribution of gas $T(r)$ in Fig. 10. As seen the distribution of $T(r)$ has a very large scatter from 10^4 K to 10^6 K. In our calculation we set the cutoff temperature for the cooling function at 10^4 K, the gas can't cool to lower temperatures.

The modeled process of SNII explosions injects to a great amount of thermal energy into the gas and generates a very large temperature scatter, also typical of our Galaxy's ISM. At each point even with crude numerical approximations a good fit can be reached for all dynamical and thermal distributions of gas and stars in a typical disk galaxy like our Galaxy.

3.3. Chemical characteristics

Fig. 11. shows the time evolution of the SFR in galaxy $SFR(t) = dM_*(t)/dt$. Approximately 90% of gas is converted into stars at the end of calculation. The most intensive SF burst happened in the first ≈ 1 Gyr, with a maximal SFR $\approx 35 M_\odot/\text{yr}$. After $\approx 1.5 - 2$ Gyr the SFR is decreases like an "exponential function" until it has a value $\approx 1 M_\odot/\text{yr}$ at the end of the simulation. To check the SF and chemical enrichment algorithm in our SPH

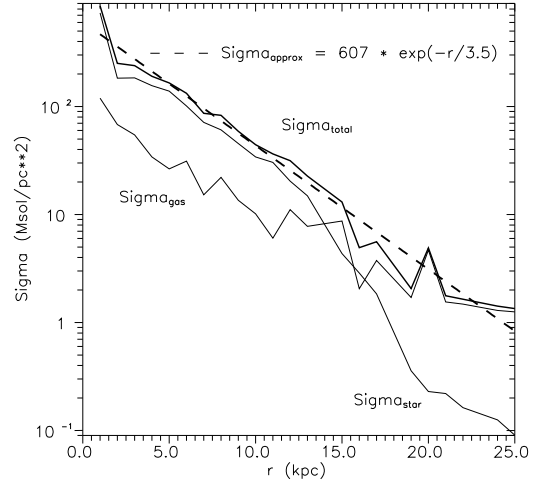


Fig. 6. $\sigma_{gas}(r)$, $\sigma_*(r)$ and $\sigma_{tot}(r) = \sigma_{gas}(r) + \sigma_*(r)$. The column density distribution in the disk of gas and stars in the final step

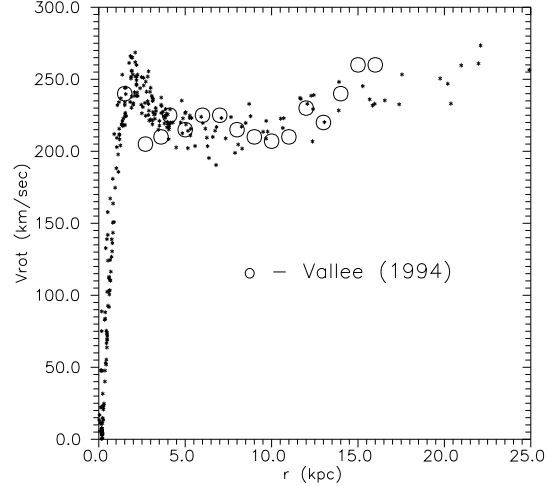


Fig. 7. $V_{rot}(r)$. The rotational velocity distribution of gas in the final step

code, we use the chemical characteristics of the disk in the "solar" cylinder ($8 \text{ kpc} < r < 10 \text{ kpc}$).

The age-metallicity relation of the "star" particles in the "solar" cylinder, $[\text{Fe}/\text{H}](t)$, is shown in Fig. 12., with observational data taken from Meusinger *et al.* (1991) and Edvardsson *et al.* (1993), while in Fig. 13. we presented the metallicity distribution of the "star" particles in the "solar" cylinder $N_*([\text{Fe}/\text{H}])$. The model data are scaled to the observed number of stars (Edvardsson *et al.* 1993). In Fig. 12. each model point represents the separate "star" particle. The mass of each "star" particle is different (from $\sim 10^4 M_\odot$ up to $\sim 2.5 \cdot 10^6 M_\odot$), because the star formation efficiency - ϵ is different in each star forming region. The model point is systematically higher than the observations (especially near the $t \approx 5$ Gyr), but if we also analyze the mass of each "star" particle we see that the

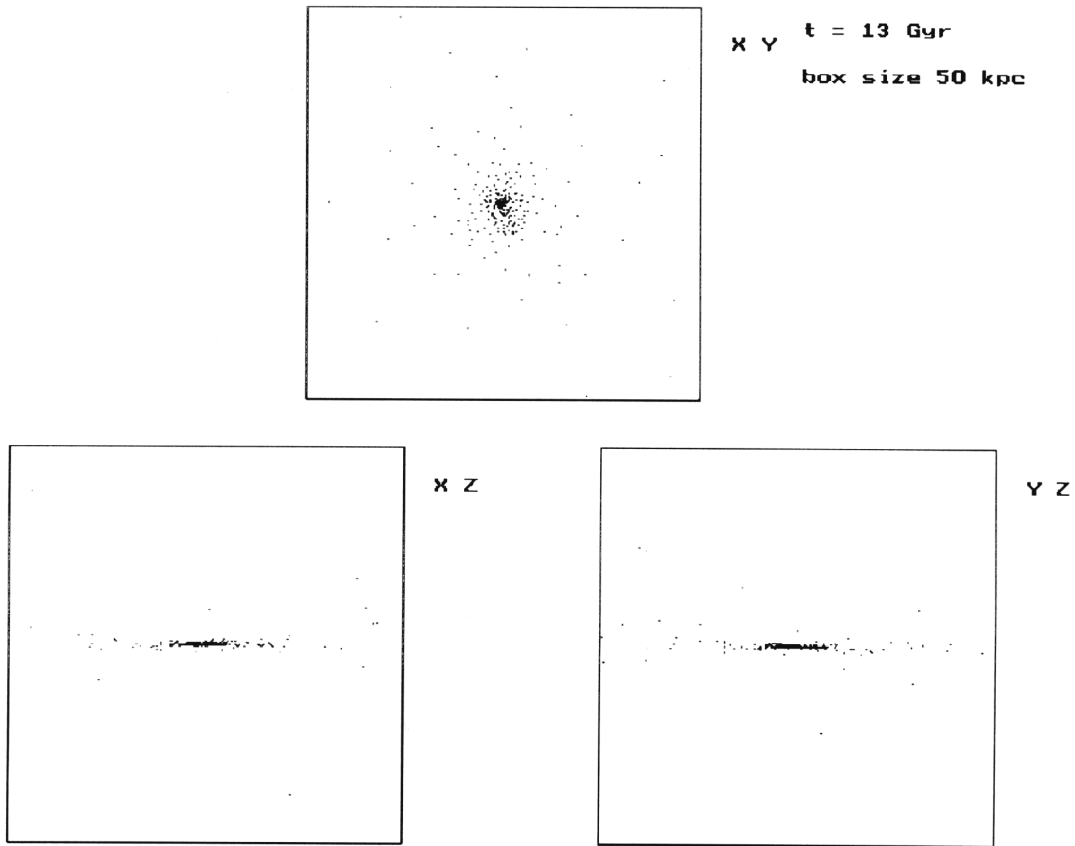


Fig. 4. The distribution of "gas" particles in the final step

more massive particles systematically show lower metallicity than the observations. If one divides the metallicity to equal zone and calculate the sum of the mass in each metallicity zone in Fig. 12. we get the results in Fig. 13. and in this figure we see what the model mass distribution has shifted to the lower metallicities.

The $[\text{O}/\text{Fe}]$ vs. $[\text{Fe}/\text{H}]$ distribution of the "star" particles in the "solar" cylinder one found in Fig. 14. In this figure we also present the observational data from Edvardsson *et al.* (1993) and Tomkin *et al.* (1992). All these model distributions are in good agreement, not only with presented observational data, but also with other data collected from Portinari *et al.* (1997).

The $[\text{O}/\text{H}]$ radial distribution $[\text{O}/\text{H}](r)$ is shown in Fig. 15. The approximation presented in the figure is obtained by a least - squares linear fit. At distances $5 \text{ kpc} < r < 11 \text{ kpc}$ the models radial abundance gradient is -0.06 dex/kpc . In the literature we found different values of this gradient defined in objects of different types. From observations of HII regions (Peimbert 1979; Shaver *et al.* 1983) we obtained oxygen radial gradient

-0.07 dex/kpc . From observations of PN of different types (Maciel & Koppen 1994) we obtained the values: -0.03 dex/kpc for PNI, -0.069 dex/kpc for PNII, -0.058 dex/kpc for PNIII, -0.062 dex/kpc for PNIIa, and -0.057 dex/kpc for PNIIb. All this agrees well with the oxygen radial gradient in our Galaxy.

3.4. Conclusion

This simple model provides a reasonable, self-consistent picture of the processes of galaxy formation and star formation in the galaxy. The dynamical and chemical evolution of the modeled disk-like galaxy is coincident with observations for our own Galaxy. The results of our modeling give a good base for a wide use of the proposed SF and chemical enrichment algorithm in other SPH simulations.

Acknowledgments. The author is grateful to S.G. Kravchuk, L.S. Pilyugin and Yu.I. Izotov for fruitful discussions during the preparation of this work. It is a pleasure to thank Pavel Kroupa and Christian Boily for comments on an earlier version of this paper. The author also thanks the anonymous referee for a helpful referee's report

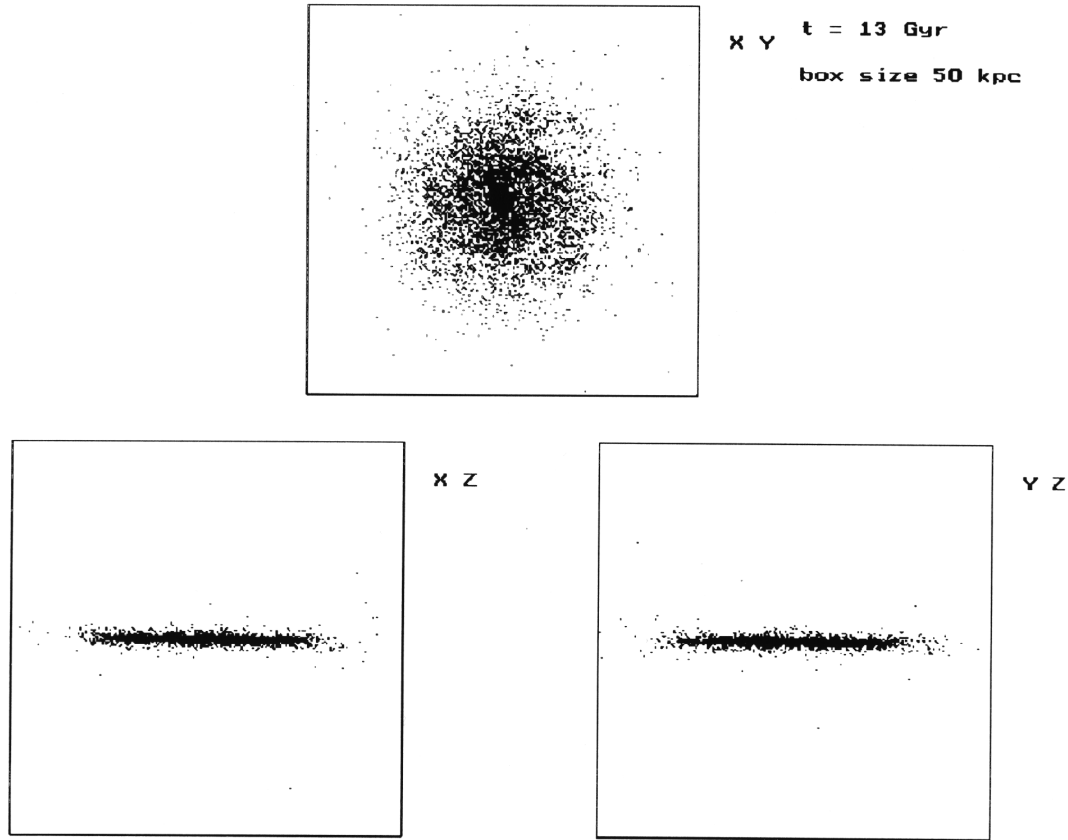


Fig. 5. The distribution of "star" particles in the final step

which resulted in a significantly improved version of this paper. This research was supported by a grant from the American Astronomical Society.

References

- Alongi M., Bertelli G., Bressan A., *et al.*, 1993, *Astron. & Astrophys. Suppl.*, **97**, 851
- Bardeen J.M., Bond J.R., Kaiser N. & Szalay A.S., 1986, *Astrophys. J.*, **304**, 15
- Bennett C.L., Boggess N.W., Hauser M.G., Mather J.C., Smoot G.F. & Wright E.L., 1993, in "The Environment and Evolution of Galaxies", Eds. Shull M.J., Thronson H.A.Jr., Kluwer Acad. Publ., 27
- Berczik P. & Kolesnik I.G., 1993, *Kinematika i Fizika Nebesnykh Tel*, **9**, No. 2, 3
- Berczik P. & Kravchuk S.G., 1996, *Astrophys. & Sp. Sci.*, **245**, 27
- Berczik P., 1998, Presented as a poster in the Isaac Newton Institute Workshop: "Astrophysical Discs", June 22 - 27, 1998, Cambridge, UK. ([astro-ph/9807059](#))
- Bertelli G., Bressan A., Chiosi C., Fagotto F. & Nasi E., 1994, *Astron. & Astrophys. Suppl.*, **106**, 275
- Bienayme O., 1998, *Astron. & Astrophys.*, **341**, 86
- Burkert A., 1995, *Astrophys. J.*, **447**, L25
- Bressan A., Fagotto F., Bertelli G. & Chiosi C., 1993, *Astron. & Astrophys. Suppl.*, **100**, 647
- Carraro G., Lia C. & Chiosi C., 1997, *Mon. Not. Roy. Astr. Soc.*, **297**, 1021
- Dalgarno A. & McCray R.A., 1972, *Annu. Rev. Astron. & Astrophys.*, **10**, 375
- Dar A., 1995, *Astrophys. J.*, **449**, 550
- Douphole B. & Colin J., 1995, *Astron. & Astrophys.*, **300**, 117
- Duerr R., Imhoff C.L. & Lada C.J., 1982, *Astrophys. J.*, **261**, 135
- Edvardsson B., Andersen J., Gustaffson B., *et al.* 1993, *Astron. & Astrophys.*, **275**, 101
- Eisenstein D.J. & Loeb A., 1995, *Astrophys. J.*, **439**, 520
- Ferriere K.M., 1995, *Astrophys. J.*, **441**, 281
- Frenk C.S., White S.D.M., Davis M. & Efstathiou G., 1988, *Astrophys. J.*, **327**, 507
- Friedli D. & Benz W., 1995, *Astron. & Astrophys.*, **301**, 649
- Greggio L. & Renzini A., 1983, *Astron. & Astrophys.*, **118**, 217
- Hernquist L. & Katz N., 1989, *Astrophys. J. Suppl. Ser.*, **70**, 419

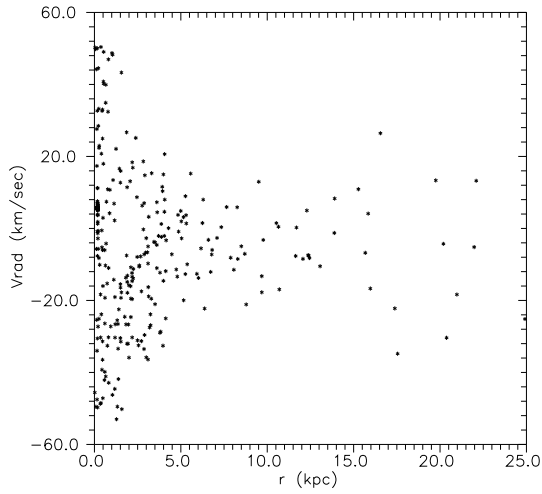


Fig. 8. $V_{rad}(r)$. The radial velocity distribution of gas in the final step

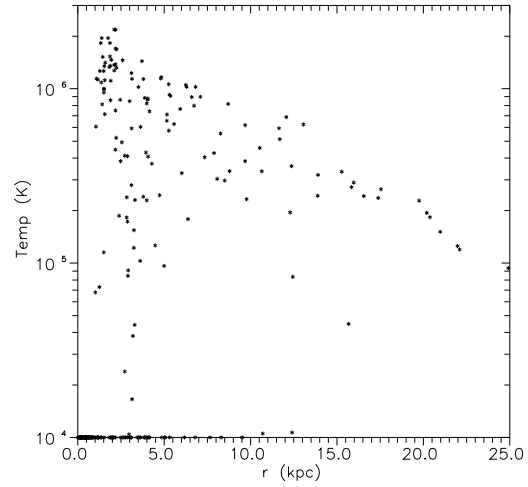


Fig. 10. $T(r)$. The temperature distribution of gas in the final step

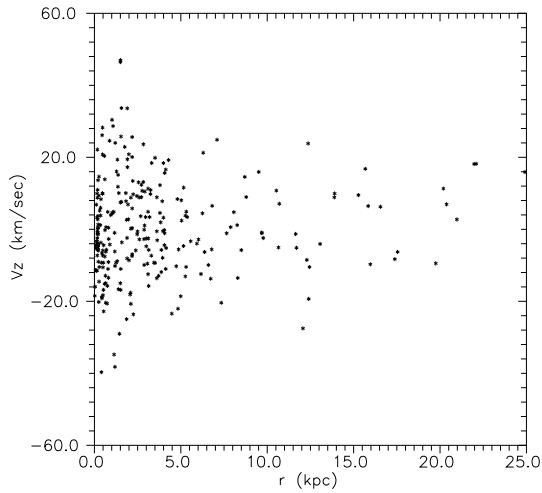


Fig. 9. $V_z(r)$. The perpendicular to disk normal velocity distribution of gas in the final step

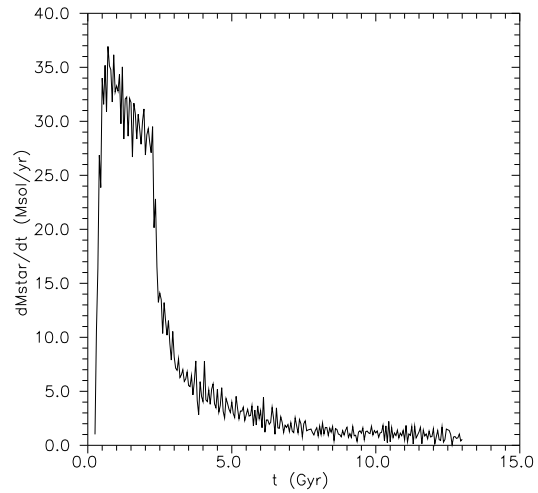


Fig. 11. $SFR(t) = dM_*(t)/dt$. The time evolution of the SFR in galaxy

Hiotelis N., Voglis N. & Contopoulos G., 1991, *Astron. & Astrophys.*, **242**, 69
 Hiotelis N. & Voglis N., 1991, *Astron. & Astrophys.*, **243**, 333
 Katz N. & Gunn J.E., 1991, *Astrophys. J.*, **377**, 365
 Katz N., 1992, *Astrophys. J.*, **391**, 502
 Kravtsov A.V., Klypin A.A., Bullock J.S. & Primack J.R., 1997, *Astrophys. J.*, **502**, 48
 Kroupa P., Tout C. & Gilmore G., 1993, *Mon. Not. Roy. Astr. Soc.*, **262**, 545
 Larson R.B., 1969, *Mon. Not. Roy. Astr. Soc.*, **145**, 405
 Leitherer C., Robert C. & Drissen L., 1992, *Astrophys. J.*, **401**, 596
 Lucy L.B., 1977, *Astron. J.*, **82**, 1013
 Maciel W.J. & Koppen J., 1994, *Astron. & Astrophys.*, **282**, 436
 Matteucci F. & Greggio L., 1986, *Astron. & Astrophys.*, **154**, 279

Mera D., Chabrier G. & Schaeffer R., 1998a, *Astron. & Astrophys.*, **330**, 937
 Mera D., Chabrier G. & Schaeffer R., 1998b, *Astron. & Astrophys.*, **330**, 953
 Meusinger H., Reimann H.G. & Stecklum B., 1991, *Astron. & Astrophys.*, **245**, 57
 Mihos J.C. & Hernquist L., 1996, *Astrophys. J.*, **464**, 641
 Monaghan J.J. & Lattanzio J.C., 1985, *Astron. & Astrophys.*, **149**, 135
 Monaghan J.J., 1992, *Annu. Rev. Astron. & Astrophys.*, **30**, 543
 Moore B., Governato F., Quinn T., Stadel J. & Lake G., 1997, *Astrophys. J.*, **499**, L5
 Nomoto K., Thielemann F.-K. & Yokoi K., 1984, *Astrophys. J.*, **286**, 644
 Navarro J.F., Frenk C.S. & White S.D.M., 1996, *Astrophys. J.*, **462**, 563

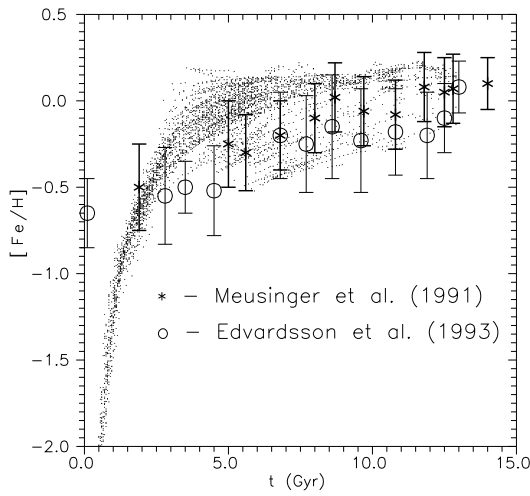


Fig. 12. $[\text{Fe}/\text{H}](t)$. The age metallicity relation of the "star" particles in the "solar" cylinder ($8 \text{ kpc} < r < 10 \text{ kpc}$)

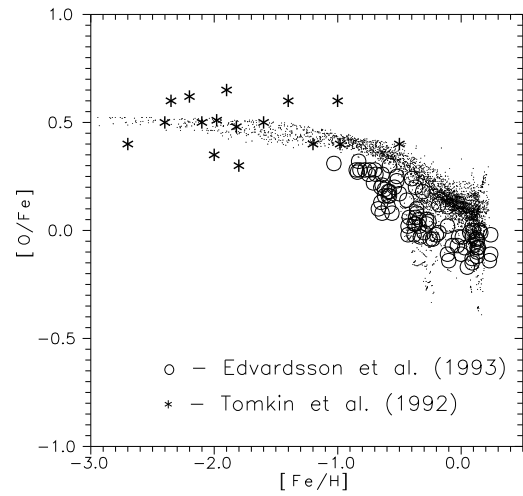


Fig. 14. The $[\text{O}/\text{Fe}]$ vs. $[\text{Fe}/\text{H}]$ distribution of the "star" particles in the "solar" cylinder ($8 \text{ kpc} < r < 10 \text{ kpc}$)

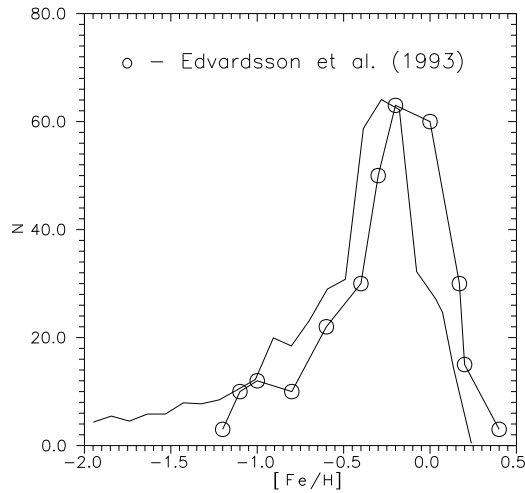


Fig. 13. $N_*([\text{Fe}/\text{H}])$. The metallicity distribution of the "star" particles in the "solar" cylinder ($8 \text{ kpc} < r < 10 \text{ kpc}$)

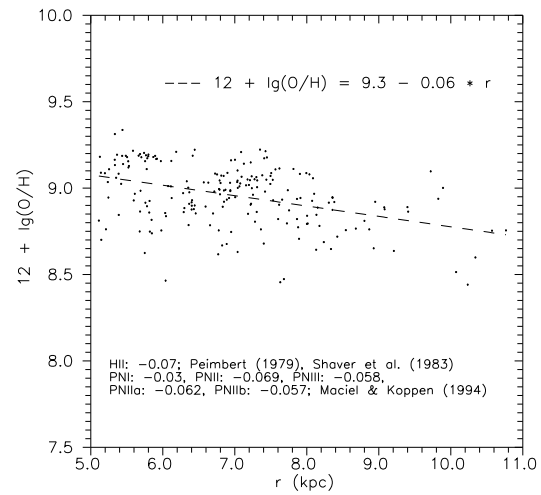


Fig. 15. $[\text{O}/\text{H}](r)$. The $[\text{O}/\text{H}]$ radial distribution

Navarro J.F., Frenk C.S. & White S.D.M., 1997, *Astrophys. J.*, **490**, 493
 Navarro J.F., 1998, *Astrophys. J.*, submitted, (astro-ph/9801073)
 Navarro J.F. & White S.D.M., 1993, *Mon. Not. Roy. Astr. Soc.*, **265**, 271
 Peebles P.J.E., 1969, *Astron. & Astrophys.*, **155**, 393
 Peebles P.J.E., 1993, in "Principles of Physical Cosmology", Princeton Univ. Press
 Peimbert M., 1979, in "The Large Scale Characteristic of the Galaxy", Ed. Burton W.B., Reidel, Dordrecht, p. 307
 Portinari L., Chiosi C. & Bressan A., 1997, *Astron. & Astrophys.*, **334**, 505
 Raiteri C.M., Villata M. & Navarro J.F., 1996, *Astron. & Astrophys.*, **315**, 105
 Renzini A. & Voli M., 1981, *Astron. & Astrophys.*, **94**, 175
 Samland M., Hensler G. & Theis Ch., 1997, *Astrophys. J.*, **476**, 544

Samland M., 1997, *Astrophys. J.*, **496**, 155
 Shaver P.A., McGee R.X., Newton L.M., Danks A.C. & Potasz S.R., 1983, *Mon. Not. Roy. Astr. Soc.*, **204**, 53
 Silk J., 1987, in IAU Symp. No. 115 "Star Forming Regions", Eds. Peimbert M., Jugaku J., Reidel, Dordrecht, p. 557
 Steinmetz M. & Muller E., 1994, *Astron. & Astrophys.*, **281**, L97
 Steinmetz M. & Muller E., 1995, *Mon. Not. Roy. Astr. Soc.*, **276**, 549
 Steinmetz M. & Bartelmann M., 1995, *Mon. Not. Roy. Astr. Soc.*, **272**, 570
 Thielemann F.-K., Nomoto K. & Yokoi K., 1986, *Astron. & Astrophys.*, **158**, 17
 Tomkin J., Lemke M., Lambert D.L. & Sneden C., 1992, *Astron. J.*, **104**, 1568
 Vallee J., 1994, *Astrophys. J.*, **437**, 179
 van den Bergh S. & McClure R.D., 1994, *Astrophys. J.*, **425**, 205

- van den Hoek L.B. & Groenewegen M.A.T., 1997, *Astron. & Astrophys. Suppl.*, **123**, 305
- Voglis N. & Hiotelis N., 1989, *Astron. & Astrophys.*, **218**, 1
- Warren M.S., Quinn P.J., Salmon J.K. & Zurek W.H., 1992, *Astrophys. J.*, **399**, 405
- Wilking B.A. & Lada C.J., 1983, *Astrophys. J.*, **274**, 698
- White S.D.M. & Rees M.J., 1978, *Mon. Not. Roy. Astr. Soc.*, **183**, 341
- White S.D.M. & Silk J., 1979, *Astrophys. J.*, **231**, 1
- Woosley S.E. & Weaver T.A., 1995, *Astrophys. J. Suppl. Ser.*, **101**, 181
- Zurek W.H., Quinn P.J. & Salmon J.K., 1988, *Astrophys. J.*, **330**, 519